Journal of Ceramic Processing Research. Vol. 13, No. 5, pp. 561~564 (2012)

J O U R N A L O F
Ceramic Processing Research

Preparation of bismuth ferrite nanopowders at different calcination temperatures

Chunlin Fu*, Meng Huo, Wei Cai and Xiaoling Deng
School of Metallurgical and Materials Engineering, Chongqing University of Science and Technology, Chongqing 401331, China

$BiFeO_3$ powders were prepared by a sol-gel process at different calcination temperatures. The DTA curve shows an obvious exothermic peak near 480.5 °C, a temperature close to the $BiFeO_3$ formation temperature, which is in agreement with the XRD result (450 °C). Having been calcined at 600 °C for 1 h, XRD spectra has the emergence of several sharp diffraction peaks in correspondence with the standard XRD spectrum of the crystalline $BiFeO_3$. As the calcination temperature was increased, the diffraction peak intensity of the XRD spectra of $BiFeO_3$ gradually was enhanced and the diffraction peaks became sharper. There is a clear endothermic peak near 825.1 °C, which is the transition temperature from the α phase to β phase and in good agreement with the reported Curie temperature. The average size of powders determined by XRD and TEM gradually increases with an increase in the calcination temperature. A shell-core structure is distinctly observed in powders calcined at 400 °C.

Key words: Bismuth ferrite, Nanopowder, Multiferroic, Sol-gel.

Introduction

Considerable interest has been aroused by multiferroic materials, which exhibit simultaneous magnetic and ferroelectric order, due to their potential applications for novel storage media and spintronic devices [1-3]. In recent years several single phase magnetoelectric multiferroics have been identified, but bismuth ferrite ($BiFeO_3$, short form BFO) is the only material presently known to express coupling between magnetic and ferroelectric order at room temperature [4-6]. Both polarization (ferroelectric) ordering with a high Curie temperature T_C of 1103 K and spin (antiferromagnetic) ordering of the G type with a magnetic transition temperature T_N of 643 K simultaneity exist in bismuth ferrite [7-9].

Nanoscale materials have been widely investigated because of their unique electrical, magnetic, and optical properties arising from their low dimensionality and quantum confinement effect [10]. Since BFO was discovered in 1960, various techniques have been successfully developed to synthesize BFO powders, such as solid-state synthesis [11], co-precipitation [9], hydrothermal synthesis [10], and sol-gel synthesis [2, 12]. In the sol-gel synthesis of BFO, the sol is usually prepared by a citric acid route [13]. In order to compensate for the evaporation loss of bismuth during the post-annealing process, an excess source of bismuth is usually added to the solution.

*Corresponding author:
Tel : +86 23 6502 3479
Fax: +86 23 6502 3706
E-mail: chlfu@126.com

In this study, BFO nanopowders were prepared at different calcination temperatures and the crystal structure and surface morphology were investigated.

Experiments

Preparation

$BiFeO_3$ powders were prepared by a sol-gel process. High-purity ferric nitrate nonahydrate ($Fe(NO_3)_3 \cdot 9H_2O$, ≥ 98.0%), bismuth nitrate ($Bi(NO_3)_3 \cdot 8H_2O$, ≥ 99.0%), nitric acid (HNO_3, ≥ 99.5%) and ethanol (C_2H_5OH, ≥ 99.7%) were used as raw materials to prepare a precursor solution. Firstly, 0.02 mol ferric nitrate nonahydrate, 0.02 mol bismuth nitrate and 100 ml ethanol were mixed for one hour. Secondly, making dilute nitric acid with the pure nitric acid and deionized water with a volume ratio of 1 : 4.8. Thirdly, 15 ml dilute nitric acid was added dropwise to a 100 ml solution of ferric nitrate nonahydrate and bismuth nitrate, and then stirred strongly to obtain a uniform and transparent sol. The sol was aged for 24 h at room temperature and then was dried in an oven at 60 °C for 48 hours to obtain the xerogel. The gel was calcined at different temperatures for 0.5 hour and ground to get $BiFeO_3$ powders.

Characterization

Thermal analyses of the dry gels were performed based on a thermal analyzer (TG-DTA, JCR-2 China) at temperatures ranging from 0 °C to 1000 °C at a heating rate of 10 K minute^{-1}. Al_2O_3 was used as a reference material and for sample holders.

X-ray diffraction (XRD, XD-3 China) was used to identify the phase of powders and the particle size of

the powders was calculated through the Scherrer formula. Transmission electron microscopy (TEM, Hitachi H-7500 Japan) was used to observe the powder surface morphology and estimate the particle size.

Results and Discussions

TG-DTA analysis

The results of thermogravimetric and differential thermal analysis (TG-DTA) of BFO dried gels are shown in Fig. 1. When the heating temperature is below 200 °C, the solvent in the dry gel is volatile, corresponding to the endothermic peak near 139.7 °C in the DTA curve. With an increase in the temperature, the exothermic peak appears near 187.7 °C, mainly due to thermal decomposition or combustion of nitrogenous substances, and the release of nitrogen gas along with 14.44% weight loss peak. When the temperature is further increased to 300 °C, the strongest exothermic peak (266.4 °C) and maximum weight loss peak (18.28%) appear, indicating that the main reaction of the dry gel occurs in the temperature range of 200 ~ 300 °C. The gaseous material mainly contains carbon dioxide, due to the decomposition and combustion of organic matter, and linear C, H, O organic molecules. The TG curve still has a small amount of weight loss within 300 ~ 480.5 °C, and then the quality of the sample no longer changed significantly with a further temperature increase, indicating that the decomposition of organics finishes before 480 °C. An obvious exothermic peak appears near 480.5 °C, a temperature close to the $BiFeO_3$ formation temperature, indicating that $BiFeO_3$ of the perovskite phase can form nanoparticles at 480.5 °C in the present experiment. There is a clear endothermic peak near 825.1 °C, which is the transition temperature of the α phase to β phase from a knowledge of the phase diagram and in good agreement with the reported Curie temperature (830 °C).

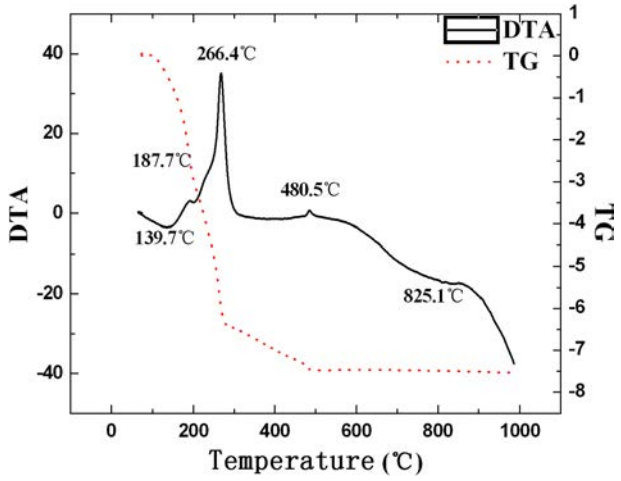

Fig. 1. TG-DTA curves of $BiFeO_3$ dry gel.

X-ray diffraction

Fig. 2 are the XRD patterns of BFO powder samples calcined at 400 °C, 450 °C, 500 °C, 600 °C, 700 °C and 800 °C for 1 h. It can be seen that the crystalline phase has appeared at 400 °C. It should be noticed that the crystalline phases are $Bi_2Fe_4O_9$ and Bi_2O_3, but no $BiFeO_3$. With an increase in the temperature, the degree of crystallinity is improved, and the phase becomes more and more complex. Powder samples calcined at 450 °C show weak diffraction peaks of the $BiFeO_3$ phase, but most of the diffraction peaks of other phases remain, indicating that the solid phase reaction already began to generate $BiFeO_3$ at this temperature. This result is in agreement with the TG-DTA analysis. Having been calcined at 600 °C for 1 h, the XRD spectrum shows the emergence of several sharp diffraction peaks, in accordance with the standard XRD spectrum of the crystal $BiFeO_3$. All of these peaks can be ascribed to the diamond-shaped distorted perovskite $BiFeO_3$, without impurity peaks. According to the standard XRD spectrum, the crystal structure of the samples are distorted perovskite structure of diamond and belong to the R3c (161) group. As the calcination temperature was increased, the diffraction peak intensity of the XRD spectra of $BiFeO_3$ gradually was improved and the diffraction peaks became sharper, indicating that the grain size gradually was enlarged.

The grain size is an important structural parameter of nanomaterials. The width of the Bragg reflection in a standard X-ray diffraction pattern provides information on the average grain size. The XRD peak broadening can measure the crystallite size in a direction perpendicular to the crystallographic plane, if the broadening arises entirely as a result of the size effect. The crystallite size can be evaluated measuring the full width at half maximum (FWHM) according to the Scherrer formula [14-16]:

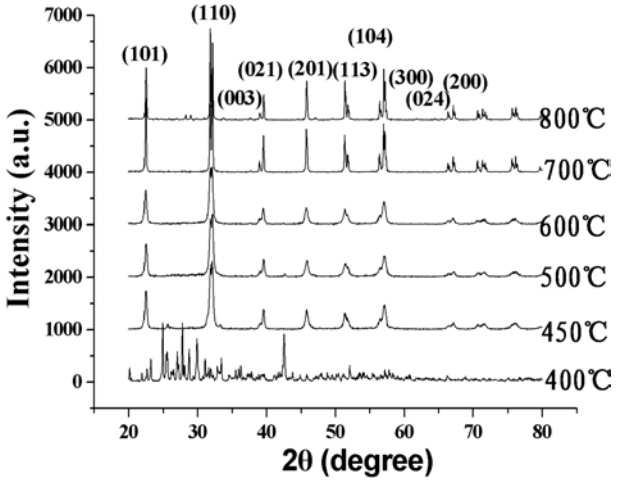

Fig. 2. XRD patterns of BFO powders calcined at different temperatures.

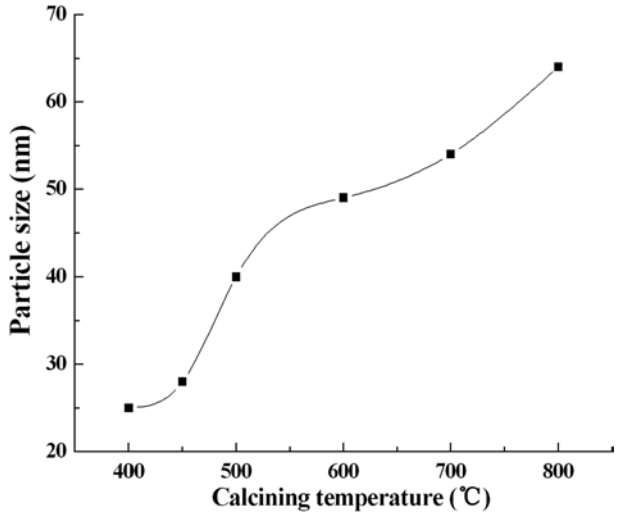

Fig. 3. Particle sizes of BFO powders calcined at different temperatures.

$$D = K\lambda / \beta \cos\theta \quad (1)$$

where D is the crystallite size (nm), K the shape factor (0.89), λ the wavelength of the X-rays ($\lambda = 1.54056$ Å for Cu Kα radiation), β the FWHM (rad) and θ the Bragg's diffraction angle (°). The average sizes of the powders calculated by Eq. 1 are shown in Fig. 3. This indicates that the particle sizes of BFO powders prepared by the sol-gel method are in the range of 25 nm and 65 nm. Moreover, the particle size gradually increases with an increase of the calcination temperature.

Transmission electron microscopy

Fig. 4 shows the TEM micrographs of the BFO powders prepared at different calcination temperatures. It can be seen that the average particle sizes of the BFO powders calcined at 400 °C, 600 °C and 800 °C are about 30 nm, 50 nm and 900 nm respectively. The results of the particle size of powders determined by XRD and TEM are similar. That is to say, the average size of powder was enlarged with an increase in the calcination temperature. However, there is an obvious difference between the numerical values of the particle sizes determined by XRD and TEM. This is probably because that the powders were dispersed incompletely before they were observed by TEM.

It is interesting that there is shell-core structure in Fig. 4(a). According to the forementioned XRD results, it can be concluded that they are Bi_2O_3 coated $Bi_2Fe_4O_9$ composites. However, Bi_2O_3 and $Bi_2Fe_4O_9$ turned into the $BiFeO_3$ phase when powders were calcined at 600 °C or 800 °C. And then, the shell-core structure vanished, as shown in Fig. 4(b) and (c).

Conclusions

In the DTA curve an obvious exothermic peak near 480.5 °C indicates that $BiFeO_3$ of the perovskite phase can form nanoparticles at 480.5 °C in the present experiment. Powder samples calcined at 450 °C show weak diffraction peaks of the $BiFeO_3$ phase, but most of the diffraction peaks of the other phases remain, indicating that the solid phase reaction already began to

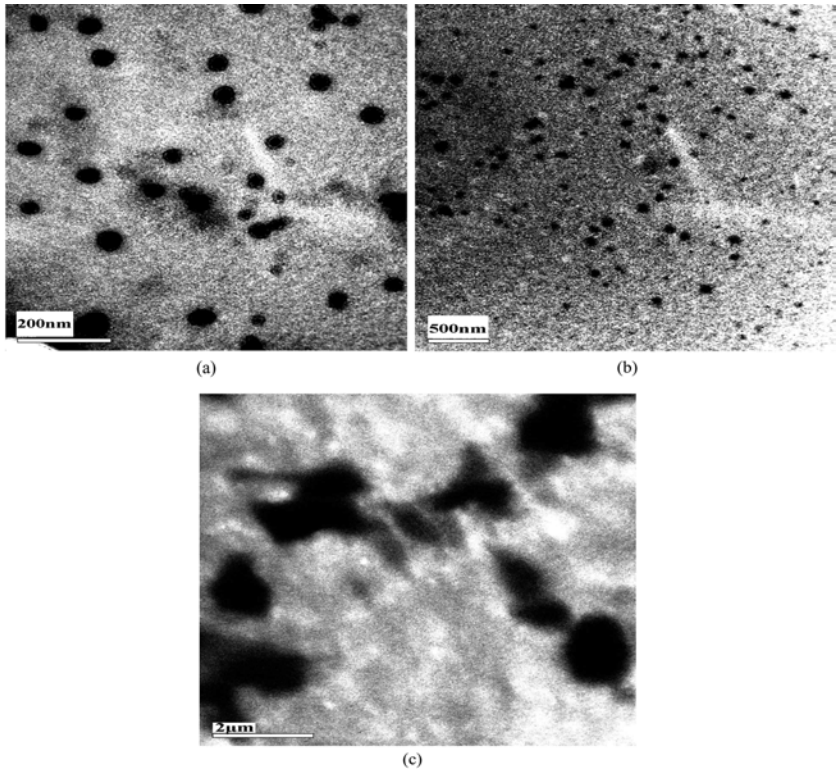

Fig. 4. TEM micrographs of BFO powders calcined at different temperatures: (a) 400 °C, (b) 600 °C, (c) 800 °C.

generate $BiFeO_3$ at this temperature. After calcining at 600 ºC for 1 h, the XRD spectrum shows the emergence of several sharp diffraction peaks, similar to the standard XRD spectrum of crystalline $BiFeO_3$. As the calcination temperature was increased, the diffraction peak intensity of the XRD spectra of $BiFeO_3$ was gradually improved and the diffraction peaks became sharper. There is a clear endothermic peak near 825.1 ºC, which is the phase transition temperature α-β from a knowledge of the phase diagram and in good agreement with the reported Curie temperature. The average size of the powder gradually increased with an increase in the calcination temperature. A shell-core structure was observed in powders calcined at 400 ºC.

Acknowledgements

This work has been supported by the National Natural Science Foundation of China (Grant No. 51102288) and Natural Science Foundation of Chongqing, China (Grant No. CSTC2011BA4027).

References

1. M. Thrall, R. Freer, C. Martin, F. Azough, B. Patterson, and R.J. Cernik, J. Eur. Ceram. Soc. 28 [13] (2008) 2567-2572.
2. A. Hardy, S. Gielis, H.V. Rul, J.D. Haen, M.K.V. Bael, and J. Mullens, J. Eur. Ceram. Soc. 29 [14] (2009) 3007-3013.
3. A. Kumar, and K.L. Yadav, Mater. Sci. Eng. B 176 [3] (2011) 227-230.
4. X. Xu, K. Seal, X. Xu, I. Ivanov, C.H. Hsueh, N.A. Hatab, L. Yin, X. Zhang, Z. Cheng, B. Gu, Z. Zhang, and J. Shen, Nano Lett. 11 [3] (2011) 1265-1269.
5. H. Jang, J.S. Lee, K.T. Ko, W.S. Noh, T.Y. Koo, J.Y. Kim, K.B. Lee, J.H. Park, C.L. Zhang, S.B. Kim, and S.W. Cheong, Phys. Rev. Lett. 106 [4] (2011) 047203.
6. A.F. García-Flores, D.A. Tenne, Y.J. Choi, W.J. Ren, X.X. Xi, and S.W. Cheong, J. Phys.- Condens. Matter. 23 [1] (2011) 015401.
7. T. Stevenson, T.P. Comyn, A. Daoud-Aladine, and A.J. Bell, J. Magn. Magn. Mater. 322 [22] (2010) 64-67.
8. S. Kazhugasalamoorthy, P. Jegatheesan, R. Mohandoss, N. V. Giridharan, B. Karthikeyan, R.J. Joseyphus, and S. Dhanuskodi, J. Alloy. Compd. 493 [1-2] (2010) 569-572.
9. A. Gajovic, S. Šturm, B. Janwar, A. Šantic, K. Zagar, and M. Cehz, J. Am. Ceram. Soc. 93 [10] (2010) 3173-3179.
10. Y. Wang, G. Xu, Z. Ren, X. Wei, W. Weng, P. Du, G. Shen, and G. Han, Ceram. Int. 34 [6] (2008) 1569-1571.
11. M. Thrall, R. Freer, C. Martin, F. Azough, B. Patterson, and R.J. Cernik, J. Eur. Ceram. Soc. 28 [13] (2008) 2567-2572.
12. J.H. Xu, H. Ke, D.C. Jia, W. Wang, and Y. Zhou, J. Alloy. Compd. 472 [1-2] (2009) 473-477.
13. A. Azam, A. Jawad, A.S. Ahmed, M. Chaman, and A.H. Naqvi, J. Alloy. Compd. 509 [6] (2011) 2909-2913.
14. S.J. Kalita, and S. Verma, Mater. Sci. Eng. C 30 [2] (2010) 295-303.
15. K.V. Rao, and C.S. Sunandana, Solid State Commun. 148 [1-2] (2008) 32-37.
16. S.B. Waje, M. Hashim, W.D. W. Yusoff, and Z. Abbas, Appl. Surf. Sci. 256 [10] (2010) 3122-3127.